Journal of New Results in Science

https://dergipark.org.tr/en/pub/jnrs

Research Article

Open Access

E-ISSN:1304-7981 https://doi.org/10.54187/jnrs.1461923

The production of B_4C reinforced metal matrix composite from waste AZ91 magnesium alloy using the ball milling method

Arife Efe Görmez[1]

Keywords:
Mg-B_4C,
High-energy ball milling,
Wear test,
Waste AZ91 magnesium Alloy,
Recycling

Abstract — In this study, the Mg/B_4C composite reinforced with boron carbide particles was produced by mechanical milling method using waste AZ91 magnesium alloy chips. The mechanical and tribological properties of the produced composites were investigated through hardness and wear tests. A mixture of AZ91 magnesium alloy chips, aluminum, and B_4C powders was milled at a rotation speed of 300 rpm with a ball-to-powder ratio of 20:1 for 3 hours. The milled powders were first cold pressed and then sintered at 550 °C for 3 hours. In density measurement, it was observed that the sample reinforced with B_4C exhibited an increase in density. In X-ray diffraction analysis, peaks corresponding to Mg, $Mg_{17}Al_{12}$, and MgO were detected, while the B_4C phase could not be identified. On the other hand, B_4C particles in the microstructure were revealed in the energy dispersive X-ray spectroscopy analysis. Scanning electron microscope images revealed that the Mg/B_4C composite had lower porosity, consistent with density measurements. It was found that the hardness and wear resistance of the Mg/B_4C composite were higher than those of the Mg alloy, which can be attributed to the presence of homogenously distributed hard B_4C particles within the microstructure.

Subject Classification (2020): 74E15, 74E30

1. Introduction

Researchers worldwide are increasingly interested in lightweight materials, such as Mg and Al, as they reduce energy consumption and greenhouse gas emissions in many engineering applications [1]. Among these materials, magnesium is a lightweight material with low density, high specific hardness, good machinability, specific strength, and high wear resistance. It can meet energy-saving and emission-reduction requirements in transportation, automotive, and aerospace applications [1-3]. In addition, Mg-based nanocrystalline and amorphous materials are very promising for hydrogen storage applications due to their low specific gravity, extraordinary hydrogen storage capacity, abundant natural resources, and cost-effectiveness [4].

The growth in manufacturing volume has undeniably led to a surge in industrial waste. However, sustainable production is the need of the hour, and manufacturers must take a step forward by adopting waste-minimizing approaches. To accomplish this, increasing the reuse of waste and using recyclable materials in the manufacturing process are highly recommended. Waste materials must be reused in the manufacturing process to avoid harming the environment. Reusing waste is cost-effective and supports sustainable manufacturing [5]. A lot of scrap or sawdust is generated during the processing or product change of magnesium alloys, which are widely used in industry. Approximately one-third of magnesium used in structural products ends up as waste, making waste reduction and sustainable production promotion critical [6]. Efficient recycling and reuse

[1]arifefe_90@hotmail.com (Corresponding Author)
[1]Department of Mathematics, Faculty of Arts and Sciences, Tokat Gaziosmanpaşa University, Tokat, Türkiye
Article History: Received: 30 Mar 2024 — Accepted: 29 Apr 2024 — Published: 30 Apr 2024

are crucial for maintaining magnesium usage and cost-effectiveness. Researchers have studied the recycling of magnesium shavings in the last few years. For example, Saleh et al. [6] successfully produced functionally graded composites using magnesium chips as matrix material by centrifugal casting. Generally, metallic chips or scraps are recycled by melting and then subjected to shaping. In the study conducted by Asgari et al., the aim was to reuse waste AZ91 magnesium alloy chips in the production of Mg-based composites. AZ91/SiC composites were produced using the stirred casting method [5]. The current literature lacks sufficient studies on the reuse of waste in MMC production, creating a significant void that must be addressed, particularly concerning Mg-based composites. By filling this gap, we can unlock valuable insights into sustainable manufacturing that benefits both the environment and industry.

Recycling technologies inevitably face significant challenges including process complexity, low efficiency, and high energy consumption [7]. Therefore, interest continues to increase for more effective recovery of magnesium chips and scrap. Thanks to powder metallurgy (P/M) recovery methods, which provide technological advantages such as low cost and eco-friendliness as an alternative to traditional casting methods, have become increasingly popular in recent years [3,7-9]. P/M manufacturing methods can produce large quantities of material with a low production temperature, which is difficult to achieve through traditional stir casting [10].

However, magnesium still has some limitations in its target application, such as low elastic modulus, ductility, and poor corrosion resistance. To overcome these challenges, magnesium is mixed with alloying elements or dopants [11]. Reinforcing elements commonly used in metal matrix composites (MMCs) are titanium diboride (TiB_2), boron carbide (B_4C), silicon carbide (SiC), alumina (Al_2O_3), boron nitride (BN), and graphite. Boron carbide (B_4C) is known as the hardest ceramic particle after cubic boron nitride (CBN) and diamond among ceramic particles [10-16]. The density of B_4C is 2.51 g/cm^3, and it has attractive properties such as high melting point, wear resistance, and high impact resistance. Additionally, B_4C is an excellent reinforcement for magnesium matrix composites [17].

Given the above developments, the method of reusing chips to create a composite material with higher value adds to the circular economy in manufacturing. To optimize waste management and reduce environmental impact, consider these factors: minimize waste and environmental impact, use resources regeneratively, and improve economic performance [18]. This can help reduce costs associated with recycling chips and enhance the quality of fabricated composite components. The B_4C-Mg/Al mixture was cold pressed after being obtained from a ball milling system. The final materials were then obtained by sintering at 550 °C. The reported approach has undergone a comprehensive quality assessment, involving testing of mechanical properties, X-ray diffraction (XRD), field emission scanning electron microscope (FESEM), and energy-dispersive X-ray spectroscopy (EDS). The findings have proven the feasibility of this approach, demonstrating how the reuse of magnesium chips' waste can improve the mechanical properties of newly produced sustainable material. These results signify a breakthrough in the quest for sustainable development and highlight the significant role that innovative approaches can play in achieving this goal.

2. Experimental

2.1. Production of B_4C-Reinforced AZ91 Magnesium Alloy Composites

In this study, AZ91 magnesium alloy chips (industrial waste), aluminum powder (27 μm, Sigma-Aldrich), and B_4C powder (<10 μm, 98%, Sigma-Aldrich) were used as starting materials for a composite product (Figure 1). Achieving the desired particle size is crucial for effective research and development. To achieve this, we used a high-energy planetary ball milling system called Retsch-PM400 to mechanically grind our powder sample. For all ball milling processes, we maintained a constant rotation speed of 300 rpm and a ball/powder ratio of 20:1. To prevent overheating, we followed a specific sequence of actions. We rotated the system clockwise for 60 seconds, waited for 20 seconds, and then turned it counterclockwise for 60 seconds. By

employing this technique, we were able to attain the desired particle size, which is necessary for accurate and reliable results. Firstly, the waste AZ91 Mg alloy chips and B_4C powder were ground together for three hours using ball milling. The current study aims to produce a composite with optimal strength and ductility by adding 6 wt.% Al powder to milled waste AZ91 Mg alloys chips/B_4C. It has been suggested that this percentage of Al content provides the best results [19, 20]. After, the new B_4C-Mg/Al mixtures were vigorously mixed in the milling system for 3 minutes to ensure the most homogeneous mixture. The resulting mixtures were then cold-pressed unidirectionally under 30 tons of pressure for 10 minutes, giving rise to a disc with a diameter of 19 mm and a thickness of 5 mm. To enhance the bonding between the materials, the cold-pressed mixtures were subjected to sintering at 550°C in a high-temperature furnace under an Argon gas atmosphere (Figure 2) for 3 hours. The sintered samples were allowed to cool in the oven. Two samples were produced: AZ91 alloy and B_4C reinforced composite. The sample weights are listed in Table 1.

Table 1. Weights of samples

Samples	Weights(g)
Mg alloys	2.575275
Mg/B_4C	2.53481

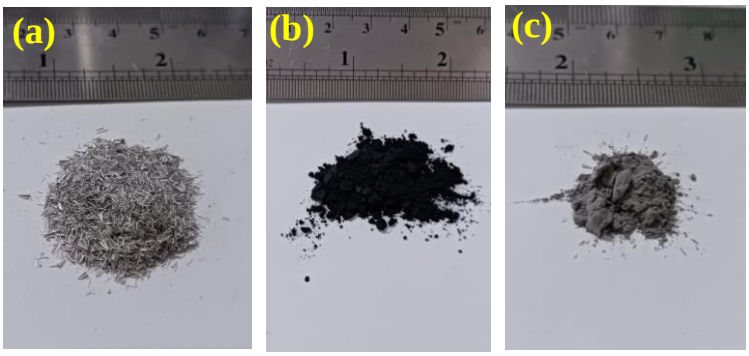

Figure 1. a) waste AZ91 magnesium alloy chips, b) B_4C powder (<10 μm, 98%) c) aluminum powder (27 μm)

Production schemes are shown in Figure 2. The produced composites are shown in Figure 3. This step was repeated twice to ensure the highest quality product. After following a series of controlled steps, we produced a composite with potential applications in various fields.

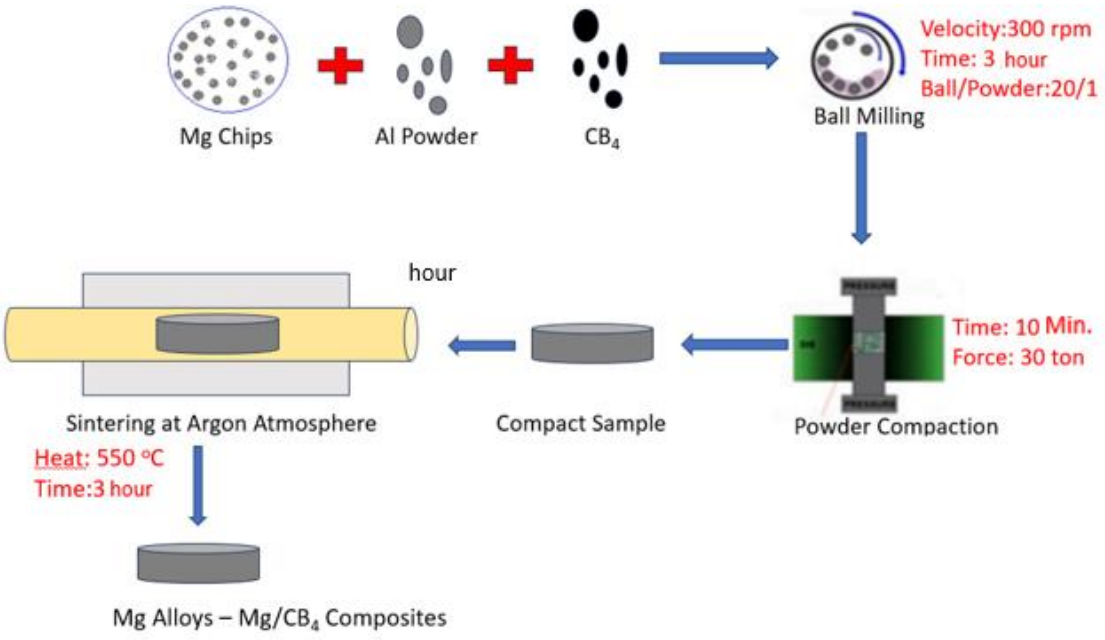

Figure 2. Production Schemes

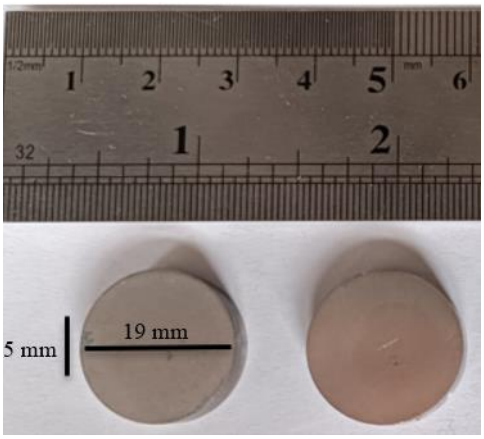

Figure 3. Produced Mg alloys and Mg/B_4C composites

2.2. Density and Porosity

The density of the samples was measured using two methods: actual density and theoretical density. The actual density was measured using Archimedes' principle, with 5 measurements taken for each sample and the average value being reported. The theoretical density was measured by dividing the mass of each sample by its volume. The final results include both the actual and theoretical densities, providing a comprehensive understanding of the density of the samples. The porosity of the samples [21] was determined by

$$P = \left(1 - \frac{\rho_a}{\rho_t}\right) 100\% \tag{2.1}$$

where ρ_a and ρ_t are the theoretical density and actual density of the samples, respectively. Three samples were measured for each material type, and the average was reported.

2.3. Hardness Test

The HWDM-3 brand microhardness tester was used to measure the microhardness of the samples under a 200 mN load. Each sample was measured 10 times, and the average was calculated.

2.4. Wear Test

Dry sliding wear tests were conducted at room temperature using a Bruker UMT tribometer device with steel pins in a pin-on-disc configuration. Disc-shaped samples measuring 19 mm in diameter and 5 mm in thickness were utilized. The wear test was performed by sliding the samples over a distance of 100 m at a sliding speed of 150 rpm under a load of 1 N. A sliding distance of 100 m was chosen to ensure that steady-state conditions were achieved. The wear diameter was set at 8 mm. The samples' surface was cleaned using acetone and an ultrasonic bath for 3 minutes to remove oil and dirt. The wear volumes were calculated by multiplying the wear area obtained from the 3D profilometer with the perimeter of the wear scar. Finally, the wear rate was determined utilizing Archard's law equation [22].

$$\frac{V}{L} = K\frac{F}{H} = kF \tag{2.2}$$

where V is the volume, L is the total sliding distance, H is the hardness, F is the applied load, K is the Archard constant, and k is the specific wear rate. Additionally, the average friction coefficient was calculated for the total distance, which provides vital information on the level of friction experienced. To determine the surface topography of the material after wear, the Bruker-Contour GT 3D Optical Profilometer was used with precision. With this technology, the surface topography of the material post-wear was determined, making it easier to understand the impact of wear on the material.

2.5. FESEM, EDX, and XRD Analyses

The process of preparing the samples involved grinding the surface with progressively finer grits of sandpaper, from 600 to 2500 mesh, followed by polishing with alumina suspension. This resulted in a gleaming, mirror-like finish on the surfaces. Subsequently, the samples were etched in a solution containing 5% nitric acid, 15% acetic acid, 20% distilled water, and 60% ethyl alcohol volumetrically for 10 seconds to achieve the desired effect. To study the structure and morphology of the samples, state-of-the-art techniques such as XRD, FESEM, and EDX were employed. The composite materials were analyzed using a QUANTA 450 FESEM and EDX equipment to determine their morphology. XRD patterns were obtained using a Cu-Kα source (λ=1.5405 Å) X-ray device to determine their elemental composition.

3. Results and Discussion

3.1. Density and Porosity

Figure 4 demonstrates the significant differences in density and porosity between AZ91 alloy and 4 wt.% B_4C reinforced composites. The data reveals that the actual density is lower than the theoretical density, indicating a lack of uniformity in the distribution of metal atoms due to inadequate compression [23]. SEM images provide unequivocal evidence for the situation at hand. A slight increase in density was observed with the addition of 4 wt.% B_4C. The increase in density with the addition of B_4C is associated with the higher density of B_4C (2.51 g/cm^3) compared to magnesium (1.8 g/cm^3).

It is possible to decrease the number of empty spaces, or "porosity", in a material by adding B_4C reinforcement to the main alloy. B_4C has a much higher density than the matrix, therefore adding 4 wt.% to the mix reduced the porosity to 3.51%. During the cold pressing process, air can get trapped between the powder grains, which increases porosity. Poor wettability between the matrix and reinforcement, and surface shrinkage during sintering can also contribute to increased porosity. This can lead to the creation of small pores that can grow larger over time [19-20].

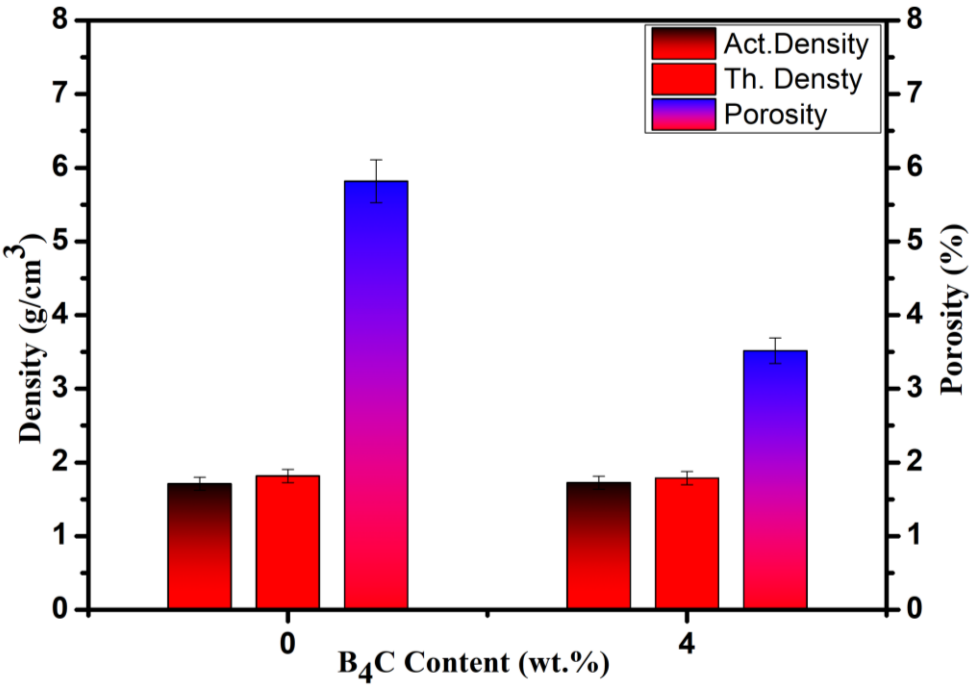

Figure 4. Variation of density and porosity with B_4C contents

3.2. XRD Analysis

Figure 5 displays XRD patterns of the base Mg alloy and composite. The Mg, $Mg_{17}Al_{12}$, and MgO diffraction peaks are visible [24]. The XRD pattern in both samples showed similar peaks with the main phases being Mg, (ICDD card 04-006-2605) $Mg_{17}Al_{12}$ (ICDD card 04-010-7477), and MgO (ICDD card 01-076-2583) [25-26]. It can be challenging to determine elements with micron-sized particles and low-weight percentages using XRD. Therefore, the peak belonging to the B_4C phase cannot be clearly distinguished [27].

The XRD patterns of the samples also showed a peak belonging to MgO, indicating slight oxidation of the samples. Mg is prone to oxidation in an oxygen-containing atmosphere, and this reaction is possible in both real and standard situations [3,14]. This has also been proven by EDX analysis.

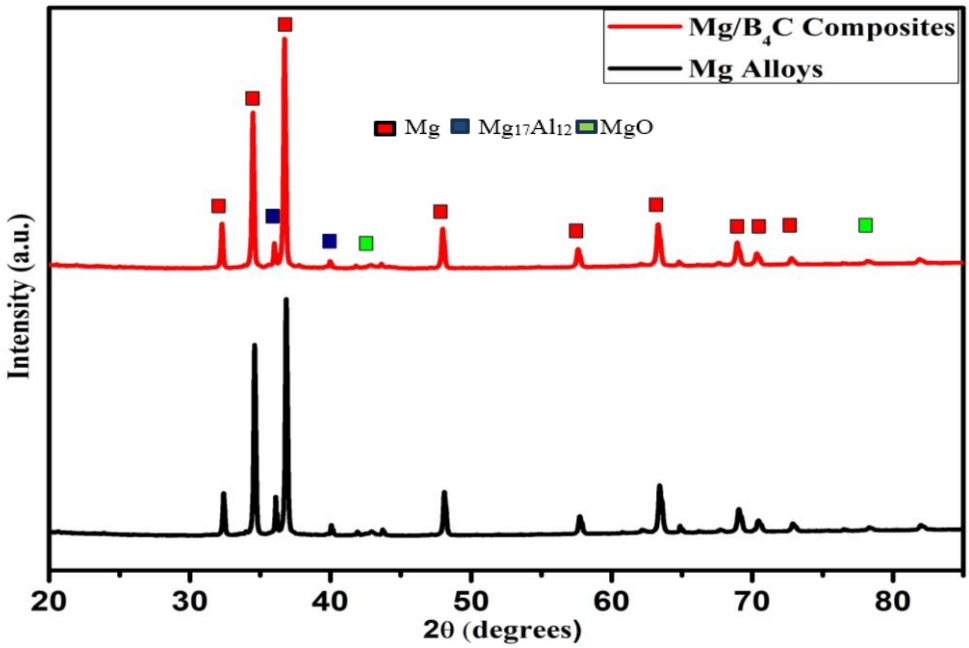

Figure 5. XRD analysis with B_4C contents

3.3. Microstructural characterization

Figure 6 a and b illustrate the FESEM images of an Mg alloy and a B_4C-reinforced composite material. In the FESEM image of the Mg alloy material, the porosity is higher than that of the B_4C-reinforced composite material (Figure 6a). The FESEM micrographs provide a clear and striking view of the compact composite structure. However, it's worth noting that the B_4C particles are not uniformly distributed on the matrix surface. According to the literature, the inhomogeneous distribution of reinforcement elements can be ascribed to the large difference in matrix and reinforcement (Mg chips-B_4C) dimensions [28]. Conducting an EDX analysis ensures accurate verification of the compositional details of both the base alloy and the composites. The results obtained from EDX are displayed in Figure 6.

All of the EDX models indicate the presence of elements from the AZ91 alloy. The presence of B_4C particles within the composite material has been confirmed by EDX analysis. Including B_4C particles increases the proportion of O in the structure, confirming the formation of MgO phases in the structure, as shown by both the EDX and XRD results. Although EDX is a highly reliable tool for elemental analysis, it may not always provide an exact weight percentage of each element, especially when the particle size is microscale, and the weight percentage is low [29]. Therefore, it is important to interpret the results carefully and consider point EDX for accurate and comprehensive elemental analysis. EDX analysis has shown that the black areas highlighted in yellow in the composite material are rich in B_4C (Figure 6b).

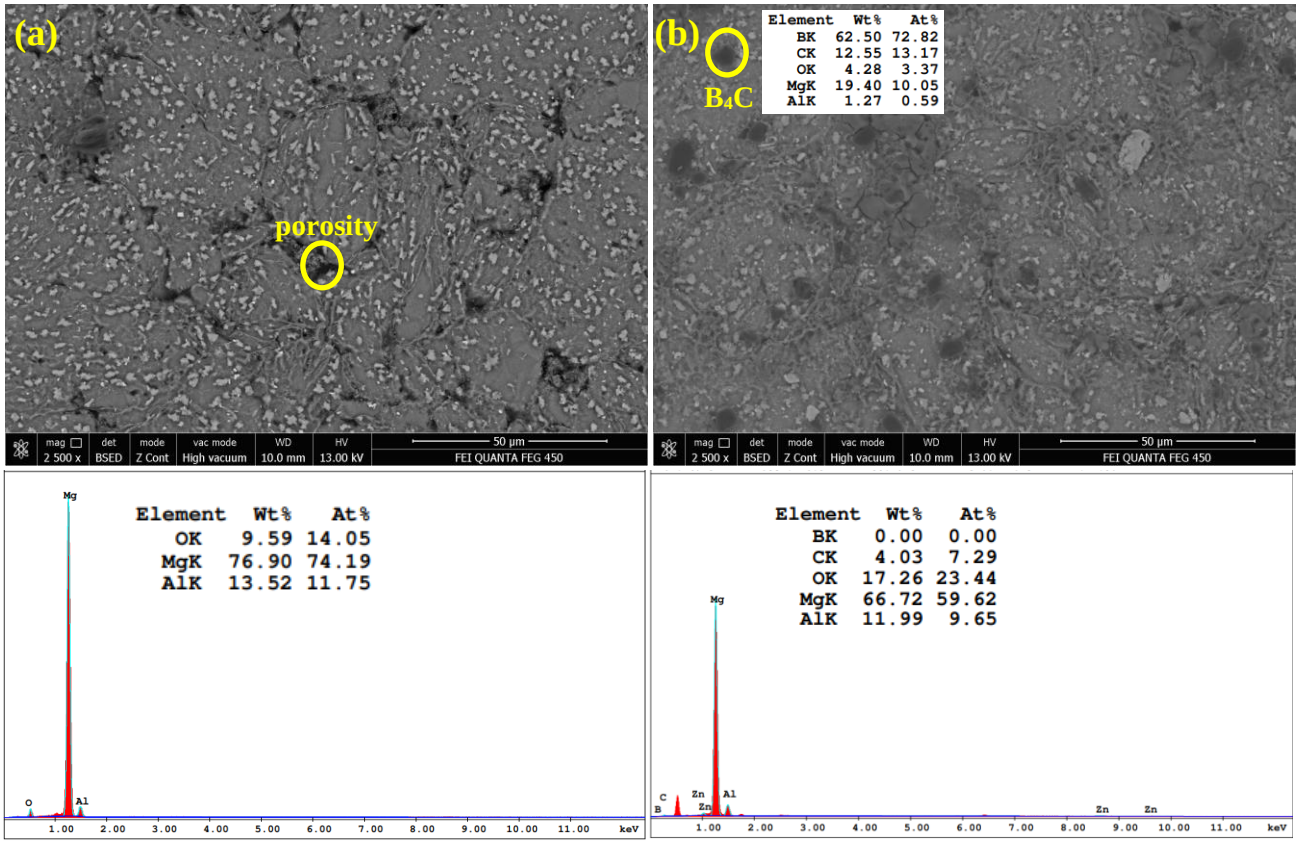

Figure 6. FESEM and EDX images of samples a) Mg alloys b) Mg/B_4C Composites

3.4. Hardness

In Table 2, the microhardness change of the samples is presented. The hardness of the B4C-doped composite increased slightly. The reason behind this could be the uniform distribution of harder B_4C particles in the matrix. Even a small amount of reinforcement can increase the composite hardness [30].

3.5. Wear Behavior

Wear tests are performed under 1 N loads and 150 rpm sliding speeds. Tablo 2 presents the wear rate of Mg-B_4C composites and base alloy with load at a sliding speed of 150 rpm. Table 2 displays the wear volumes calculated by multiplying the area in the picture and the perimeter of the wear mark. A slight increase has been observed in the wear rate of Mg-B_4C composite compared to the base alloy. Composites are highly effective in resisting surface damage, thanks to the presence of a hard ceramic phase that acts as an impenetrable barrier against asperities from a hard counter surface. It's a fact that frictional heating causes an increase in the surface temperature of a pin. Thermal softening causes plastic deformation in the base alloy when the surface temperature increases. It's worth noting that in the composites featured in Figure 6, B_4C particles have a clear advantage over the base alloy. They effectively delay the thermal effect and enable the easy formation of the oxidized layer. Accordingly, composites show a modest increment in wear rate. The addition of B_4C increased the wear volume and rate. It is worth noting that materials with higher hardness have better wear and abrasion resistance, but the contact surface may get damaged due to wear [6].

In Figure 7 (a-b), you can observe the change in the coefficient of friction (COF) and the 3D profilometer graphs, depending on the B_4C content of the composites. Table 2 lists the average COF values of Mg alloy and B_4C-reinforced composite materials as 0.31687 and 0.3843, respectively. It has been observed that the composites exhibit superior friction properties compared to the AZ91-based alloy. However, boron carbide particles were found to increase the coefficient of friction. Similar results have been previously reported for other supplements [28, 29-31].

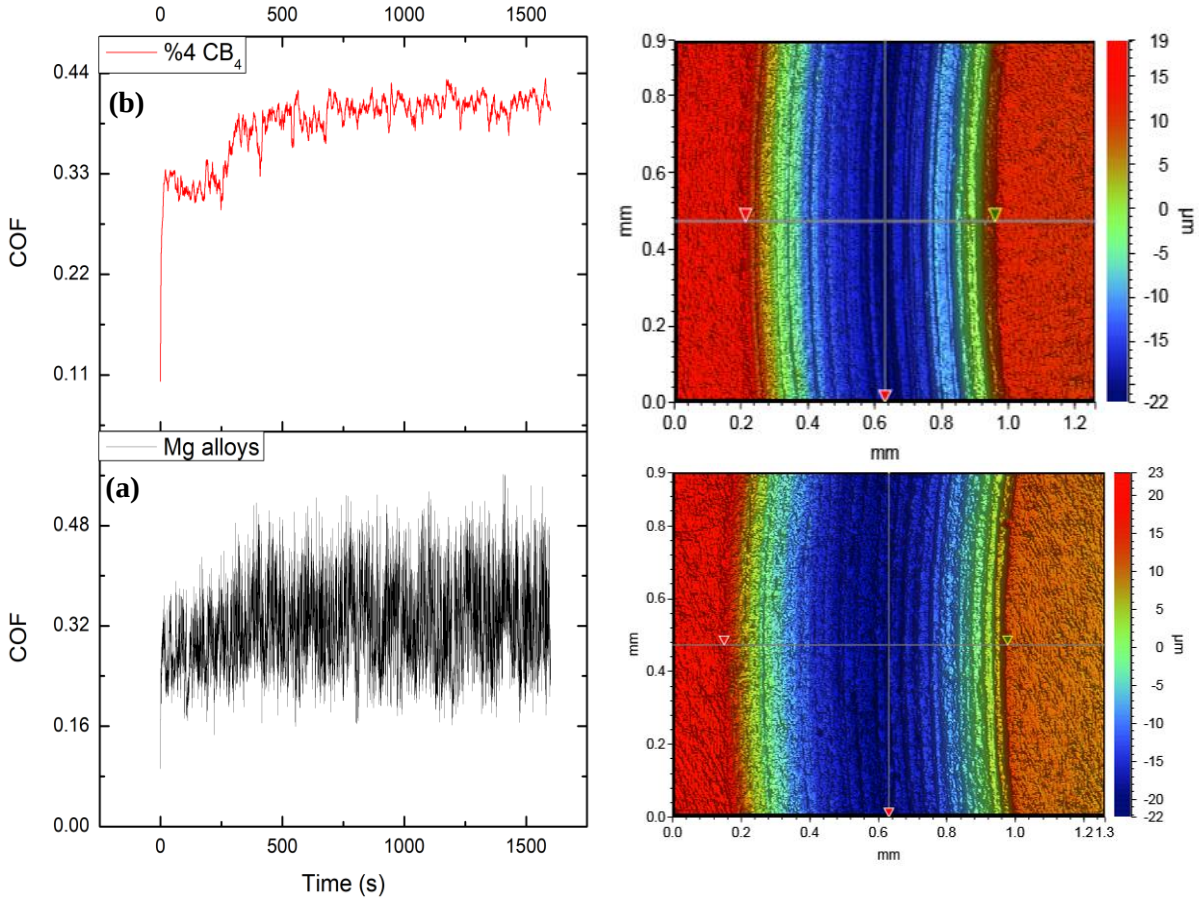

Figure 7. COF and 3D profilometer with B_4C contents

Table 2. Hardness, average COF, wear volume, and wear rate values of samples a) Mg alloys b) Mg/B_4C Composites

Samples	Hardness ($HV_{0.2}$)	Average COF	Wear Volume (mm^3)	Wear Rate (mm^3/N.m)
Mg alloys	87.48	0.31687	0.21488	0.00215
Mg/ B_4C Composites	89.4	0.3843	0.23926	0.00239

4. Conclusion

This study uses the powder metallurgy production method to produce B_4C reinforced metal matrix composite from waste AZ91 magnesium alloy. Below are the conclusions reached.

i. Metal matrix composite from waste AZ91 magnesium alloy chips reinforced with boron carbide particles was successfully produced by ball milling, cold pressing, and sintering.

ii. Reusing the magnesium chips formed during machining processes as matrix material can reduce sawdust waste, which is a negative situation in production.

iii. In FESEM and EDX analysis, it was observed that B_4C particles were distributed inhomogeneously in MMCs. The penetration of the element creates a good combination between the B_4C dopant particle and the Mg matrix.

iv. All of the EDX models indicate the presence of elements from the AZ91 alloy. The presence of B_4C particles within the composite material has been confirmed by EDX analysis. Including B_4C particles increases the proportion of O in the structure, confirming the formation of MgO phases in the structure, as shown by both the EDX and XRD results.

v. The XRD pattern in both samples showed similar peaks with the main phases being Mg, $Mg_{17}Al_{12}$, and MgO.
vi. Density and hardness increased with B_4C supplementation. Porosity in the structure has decreased.
vii. B_4C supplementation increased wear rate and wear volume. COF increased.

Author Contributions

The author read and approved the final version of the paper.

Conflict of Interest

The author declares no conflict of interest.

Acknowledgment

This study was supported by TÜBİTAK, Grant number: 121C516.

References

[1] G. S. Arora, K. K. Saxena, *A review study on the influence of hybridization on the mechanical behavior of hybrid Mg matrix composites through powder metallurgy*, Materials Today: Proceedings, 2023 (2023) Article Number 217 6 pages.

[2] C. Tang, Y. Zhang, P. Li, H. Huang, J. Zhang, *The microstructure and mechanical properties of multicomponent Mg/Al/Ce-LDO nanoparticle reinforced Mg matrix composite*, Journal of Alloys and Compounds 981 (2024) Article ID 173676 7 pages.

[3] S. J. Huang, A. Abbas, B. Ballóková, *Effect of CNT on microstructure, dry sliding wear and compressive mechanical properties of AZ61 magnesium alloy*, Journal of Materials Research and Technology 8 (5) (2019) 4273–4286.

[4] M. Gogebakan, I. Karteri, B. Avar, C. Kursun. *Crystallization behavior of Mg–Cu–Y amorphous alloy*, Journal of Thermal Analysis and Calorimetry, 110 (2) (2012) 793-798.

[5] A. Asgari, M. Sedighi, P. Krajnik. *Magnesium alloy-silicon carbide composite fabrication using chips waste.* Journal of Cleaner Production 232 (2019) 1187-1194.

[6] B. Saleh, A. Ma, R. Fathi, N. Radhika, B. Ji, J. Jiang, *Wear characteristics of functionally graded composites synthesized from magnesium chip waste*, Tribology International 174 (2022) Article ID 107692 14 pages.

[7] H. Zhao, T. Yu, C. Zeng, W. Peng, Z. Sun, H. Hu, *Microstructure and mechanical properties of steel wire reinforced Mg matrix composites fabricated by composite extrusion*. Composites Communications, 43 (2023) Article ID 101711 6 pages.

[8] M. Hu, Z. Ji, X. Chen, and Z. Zhang, *Effect of chip size on mechanical property and microstructure of AZ91D magnesium alloy prepared by solid-state recycling*, Materials Characterization 59 (4) (2008) 385-389.

[9] D. H. Li, M. L. Hu, H. B. Wang, W. A. Zhao, *Low-temperature mechanical property of AZ91D magnesium alloy fabricated by solid recycling process from recycled scraps*, Transactions of Nonferrous Metals Society of China 21 (6) (2011) 1234–1240.

[10] Q. C. Jiang, H. Y. Wang, B. X. Ma, Y. Wang, F. Zhao, *Fabrication of B_4C participate reinforced magnesium matrix composite by powder metallurgy*, Journal of Alloys and Compounds 386 (1–2) (2005) 177–181.

[11] L. Poovazhagan, K. Kalaichelvan, A. Rajadurai, V. Senthilvelan, *Characterization of hybrid silicon carbide and boron carbide nanoparticles-reinforced aluminum alloy composites*, Procedia Engineering, 143 (2013) 681–689.

[12] M. Uzun, M. S. Çetin. *Investigation of characteristics of Cu-based, Co-Cr-C reinforced composites produced by powder metallurgy method*, Advanced Powder Technology 32 (6) (2021) 1992-2003.

[13] M. Dhanashekar, P. Loganathan, S. Ayyanar, S. R. Mohan, T. Sathish, *Mechanical and wear behavior of AA6061/SiC composites fabricated by powder metallurgy method*, Materials Today: Proceedings (2020) 1008–1012.

[14] B. Yucel. *High temperature sliding wear behavior of Inconel 617 and Stellite 6 alloys*, Wear 269 (9-10) (2010) 664-671.

[15] S. Kumar, V. Subramanya Sarma, B. S. Murty. *High-temperature wear behavior of Al–4Cu–TiB_2 in situ composites.* Wear 268 (11-12) (2010) 1266-1274.

[16] Y. Gaylan, B. Avar, M. Panigrahi, B. Aygün, A A. Karabulut, *Effect of the B_4C content on microstructure, microhardness, corrosion, and neutron shielding properties of Al–B_4C composites*, Ceramics International 49 (3) (2023) 5479-5488.

[17] M. Khakbiz, F. Akhlaghi. *Synthesis and structural characterization of Al–B_4C nano-composite powders by mechanical alloying*, Journal of Alloys and Compounds 479 (1-2) (2009) 334-341.

[18] M. Lieder, A. Rashid. *Towards circular economy implementation: a comprehensive review in the context of the manufacturing industry.* Journal of Cleaner Production 115 (2016) 36-51.

[19] M. A. Thein, L. Lu, M. O. Lai. *Effect of milling and reinforcement on mechanical properties of nanostructured magnesium composite*, Journal of Materials Processing Technology 209 (9) (2009) 4439-4443.

[20] H. Sharifi, V. Eidivandi, M. Tayebi, A. Khezrloo, E. Aghaie, *Effect of SiC particles on thermal conductivity of Al-4%Cu/SiC composites,* Heat and Mass Transfer/Waerme- und Stoffuebertragung 53 (12) (2017) 3621–3627.

[21] A. Hossein, R. Ebrahimifard, M. A. Baghchesara. *Investigation of microstructure and mechanical properties of nano MgO reinforced Al composites manufactured by stir casting and powder metallurgy methods: A comparative study*. Composites Part B: Engineering 56 (2014) 217-221.

[22] J. F. Archard and J. F. A. Charj, *Contact, and Rubbing of Flat Surfaces,* Journal of Applied Physics 24 (8) (1953) 981–988.

[23] H. R. Ezatpour, M. Torabi-Parizi, S. A. Sajjadi. *Microstructure and mechanical properties of extruded Al/Al_2O_3 composites fabricated by stir-casting process*. Transactions of Nonferrous Metals Society of China 23 (5) (2013) 1262-1268.

[24] R. Zhao, J. Pei, W. Du, Z. Zhao, L. Zhang, J. Gao., D. Tie, *Fabrication of magnesium-coated graphene and its effect on the microstructure of reinforced AZ91 magnesium-matrix composites*, Advanced Composites and Hybrid Materials 5 (2022) 504-512.

[25] Y. Zhuang, H. Wang, H. Li, L. Zheng, J. Li, P. Zhou, *Synergistic effect of grain size, β-$Mg_{17}Al_{12}$, and texture on mechanical properties of Mg-15Al (wt.%) magnesium alloy processed by equal channel angular pressing*, Journal of Materials Engineering and Performance 29 (2020) 4360-4369.

[26] S. G. Moga, D. A. Negrea, C. M. Ducu, Malinovschi, V., Schiopu, A. G., Coaca, E., Patrascu, I. *The influence of processing time on morphology, structure and functional properties of PEO coatings on AZ63 magnesium alloy*, Applied Sciences 12 (24) (2022) Article Number 12848.

[27] H. Mindivan, A. Efe, A. H. Kosatepe, E. S. Kayali, *Fabrication and characterization of carbon nanotube-reinforced magnesium matrix composites,* Applied Surface Science 318 (2014) 234-243.

[28] A. C. Stone, P. Tsakiropoulos, *Characterisation of the spatial distribution of reinforcement in powder metallurgy route Al/SiCp metal matrix composites*, Materials Science and Technology 11 (3) (1995) 222–227.

[29] S. Banerjee, S. Poria, G. Sutradhar, P. Sahoo, *Dry sliding tribological behavior of AZ31-WC nano-composites*, Journal of Magnesium and Alloys 7 (2) (2019) 315-327.

[30] Q. B. Nguyen, Y. H. M. Sim, M. Gupta, C. Y. H. Lim, *Tribology characteristics of magnesium alloy AZ31B and its composites*, Tribology International 82 (2015) 464-471.

[31] H. Mindivan, A. Efe, E. S. Kayali, *Hot extruded carbon nanotube reinforced magnesium matrix composites and its microstructure, mechanical, and corrosion properties*, Magnesium Technology (2016) 429-433.